Soft Matter

Accepted Manuscript

ROYAL SOCIETY OF CHEMISTRY

www.rsc.org/softmatter

ARTICLE TYPE www. rsc.org/xxxxxx | XXXXXXXX

The effect of links on the interparticle dipolar correlations in supramolecular magnetic filaments

Pedro A. Sánchez,*[a‡] Joan J. Cerdà,[b] Tomás M. Sintes,[b] Alexey O. Ivanov[c], and Sofia S. Kantorovich[ac]

Received Xth XXXXXXXXXX 20XX, Accepted Xth XXXXXXXXX 20XX
First published on the web Xth XXXXXXXXXX 200X
DOI: 10.1039/b000000x

We present a combined computational and analytical study of supramolecular magnetic filaments, *i.e.* permanently linked chains of ferromagnetic nanocolloids. We put forward two different models for the interparticle connectivity within the chain. In the first model, the magnetic dipoles of the particles are free to rotate independently from the permanent links. The second model penalises the misalignment of the dipoles by coupling their orientations to the chain backbone. We show that the effect of the long-range magnetic dipolar interactions on the zero field net magnetic moment of the chain becomes less significant in the second case. However, the overall magnetic response in the model of freely rotating dipoles is much weaker.

1 Introduction

Magnetic fluids—ferrofluids and magnetorheological fluids—are usually created by adding independent micron or submicron sized magnetic particles to a carrier fluid to form a colloidal suspension. These magnetic systems have been studied theoretically and experimentally for more than forty years.[1–3] Among the factors that determine the physical properties of such systems, the self-assembly of their magnetic colloids into chains, rings and branched structures by effect of the magnetic dipolar interactions has turned out to be crucial.[4–7]

In general, the control of self-assembly has proven to be a key tool with which to tune the macroscopic properties of soft matter. Numerous systems based on this approach have been studied in recent years, such as patchy colloids,[8–10] blunt end DNA duplexes,[11–14] and magnetorheological suspensions.[15,16] Self-assembled structures can be further stabilised and/or modified by adding other bonding mechanisms to the system. This allows the creation of supramolecular structures with specific properties, for example, magnetic gels[17–19] and DNA origami structures.[20–22]

In magnetic soft matter, self-assembly is mainly influenced by the anisotropic and long-range nature of the magnetic dipolar interaction. In particular, this interaction favors the aggregation of the colloids of a magnetic fluid into linear chains, with a head-to-tail arrangement of the dipolar moments. The formation of these self-assembled dipolar chains can be stimulated and controlled by the application of external magnetic fields. Once a self-assembled chain has been formed, it can be structurally stabilised by adding permanent molecular crosslinks between the neighbouring particles. The result of this procedure is a permanent polymer-like chain of magnetic colloids that keeps its linear structure under a broad range of environmental conditions.[23–27] These systems, known as a supramolecular magnetic filaments, are the main subject of our study. An alternative experimental method to create magnetic filaments is the *in situ* crystalline growth of magnetic beads at specific spots along the monomer sequence of a linear polymer.[28] In general, the advances in experimental techniques that have taken place during the last decade are leading to a higher control of the structure and properties of magnetic filaments, making possible the creation of stable permanent chains with increasing degrees of flexibility and aspect ratios.

To date, most of the research efforts on magnetic filaments have been devoted to their application as magnetoresponsive actuators and propellers in micro- and nano-fluidic systems.[29–33] Nevertheless, these systems seem to be promising building blocks for various technologies.[34] One of the most interesting and still unexplored potential applications of magnetic filaments is their use as a replacement of the independent magnetic colloids present in conventional magnetic fluids. The permanent chain structure of the filaments is expected to have a significant impact on the magnetic, optical and rheological properties of such fluids, particularly at high temperatures, when the dipolar chain self-assembly is suppressed by the thermal fluctuations. Furthermore, magnetic filaments are expected to have a higher resistance to shear stress. Finally, they are likely to be more responsive to external mag-

[a] *Faculty of Physics, University of Vienna. Boltzmanngasse 5, 1090 Vienna, Austria.*
‡ *E-mail: pedro.sanchez@univie.ac.at*
[b] *Instituto de Física Interdisciplinar y Sistemas Complejos, IFISC (CSIC-UIB). Universitat de les Illes Balears. E-07122 Palma de Mallorca, Spain.*
[c] *Institue of Mathematics and Computer Sciences, Ural Federal University. Lenin av. 51, Ekaterinburg, 620083, Russia.*

netic fields due to the persistent prealignment of the particles. Despite the interest that such prospective characteristics have for technological applications, to the best of our knowledge, no studies devoted to the fundamental understanding of magnetic fluids made out of magnetic filaments have been performed so far. This work represents the first step to address this topic. In particular, we focus on the characterisation of the zero field net magnetic moment of a single isolated filament, paying special attention to the effect of the permanent links between neighbouring particles. To this extent, we use two different linking approaches. In the first case, we connect the centres of neighbouring particles with an isotropic bonding potential, without restricting particle rotations. In the second case, the interparticle bonding potential is considered to be angular-dependent and hinders the rotation of the dipoles with respect to their head-to-tail orientation. Employing Langevin dynamics simulations and analytical theory, we describe the intrachain dipole-dipole correlations and predict the zero field magnetic response. It turns out that in the case of the freely rotating dipoles, the role of the long-range nature of the dipolar interactions, enhanced by the spatial alignment of particles, is much more significant than in the second case. Importantly, in both cases magnetic filaments exhibit significantly higher correlations than that of self-assembled ferroparticle chains, especially at high temperatures.

The article is organised as follows: in Section 2 we discuss in detail the models of magnetic filaments chosen for this study. Section 3 describes our theoretical approaches, as well as the simulation methods. In Section 4 the main results of the study are discussed, and concluding remarks are presented in Section 5.

2 Magnetic filaments modelling

Supramolecular nature and polymer-like chain structure of magnetic filaments suggest the use of coarse-grained bead-spring models as a convenient approach to capture the fundamental physics of these systems.[35,36] In this Section we describe the models of magnetic filaments we used, by first introducing their common ingredients before discussing separately the details of the two different particle linking mechanisms.

2.1 Bead-spring modelling approach: common ingredients

For simplicity, we only consider magnetic filaments formed by monodisperse magnetic colloids. The latter are modelled as identical spherical beads with a characteristic diameter σ and a point magnetic dipole moment $\vec{\mu}$ located at their centre. Therefore, the long-range magnetic interactions between the beads are described by the conventional dipole-dipole pair potential:

$$U_{dd}(\vec{r}_{ij};\vec{\mu}_i,\vec{\mu}_j) = \frac{\vec{\mu}_i\cdot\vec{\mu}_j}{r^3} - \frac{3\,[\vec{\mu}_i\cdot\vec{r}_{ij}]\,[\vec{\mu}_j\cdot\vec{r}_{ij}]}{r^5}, \qquad (1)$$

where $r = \left\|\vec{r}_{ij}\right\|$, being $\vec{r}_{ij} = \vec{r}_i - \vec{r}_j$ the displacement vector connecting the centres of beads i and j with dipolar moments $\vec{\mu}_i$ and $\vec{\mu}_j$ respectively. Another relevant interaction between the spherical beads is the isotropic steric repulsion, which we model by means of a Weeks-Chandler-Andersen pair potential (WCA),[37]

$$U_{\mathrm{WCA}}(r) = \begin{cases} U_{\mathrm{LJ}}(r) - U_{\mathrm{LJ}}(r_{cut}), & r < r_{\mathrm{cut}} \\ 0, & r \geq r_{\mathrm{cut}} \end{cases}, \qquad (2)$$

where $U_{\mathrm{LJ}}(r)$ is the conventional Lennard-Jones potential,

$$U_{\mathrm{LJ}}(r) = 4\varepsilon_s[(\sigma/r)^{12} - (\sigma/r)^6], \qquad (3)$$

and $r_{\mathrm{cut}} = 2^{1/6}\sigma$ is the shifting parameter that makes the potential purely repulsive. Therefore, as mentioned above, the dipolar beads have a characteristic volume defined by their diameter, σ, but the steric repulsion between them is actually a soft core that does not impose a strict bound to the minimum centre-to-centre distance. In practice, the typical separation between neighbouring beads will be determined by the balance between all of the relevant attractive and repulsive forces. The choice of a soft core potential for the excluded volume of the magnetic beads is firstly imposed by the simulation method, but it is also physically grounded; even though the magnetic materials used to make dipolar colloids are typically rigid solids at working conditions, in most cases the particles are stabilised by soft polymer shells.[26,27,38]

In this work, all the physical parameters of the system are measured in reduced units: the reduced characteristic diameter of the colloids is $\sigma = 1$, their reduced mass $m = 1$, and the prefactor of the reduced steric potential (2) is $\varepsilon_s = 1$.

2.2 Chain connectivity Model 1: free rotating dipoles model

A very simple bead-spring modelling approach to represent the permanent chain connectivity of the magnetic colloids consists of adding an isotropic confining pair potential between first-nearest neighbours. In this model, we chose to bond adjacent beads in the chain by means of a finitely extensible nonlinear elastic potential (FENE), which can be defined as a function of the centre-to-centre distance, r, as:

$$U_{\mathrm{FENE}}(r) = \frac{-K_f}{2}\,\ln\left[1 - \left(\frac{r}{r_f}\right)^2\right], \qquad (4)$$

where we take $r_f = 1.5\sigma$ and $K_f = 30$. In our previous studies,[35,39] these parameters kept the effective separation between the first-nearest neighbours close to the reference value

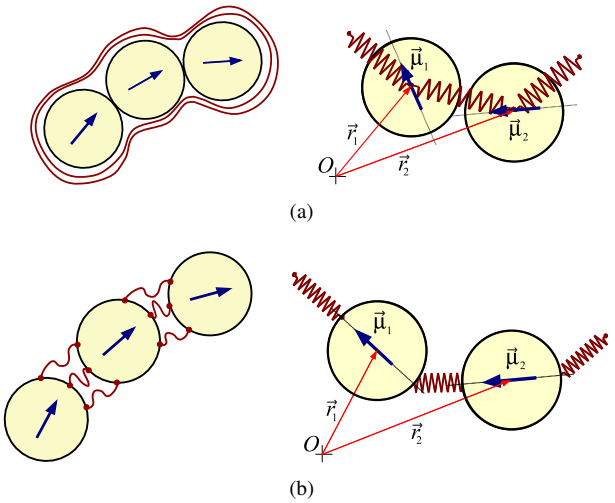

Fig. 1 Schematic representations of the two different bead-spring models of magnetic filaments used in this work (right) and their corresponding physical mechanisms for keeping the chain connectivity (left). Dipole moments are depicted as arrows, and connectivity mechanisms as curved or zigzag lines. (a) Model 1: free rotating dipoles model. (b) Model 2: bond-dipole coupling model. See the main text for further details.

$\sigma = 1$. Figure 1(a) shows a scheme of this modelling approach together with a sketch of the physical chain connectivity mechanism that it may represent. Specifically, the model does not impose any particular restriction on the rotation of the beads and, as such, on the rotation of their associated point dipoles. The FENE potential acts like a spring whose ends are attached to the centres of the linked beads, keeping them in close contact but putting no penalty on their rotations. Therefore, the dipoles will adopt a head-to-tail configuration simply by the cooperative influence of the magnetic field generated by their neighbours and/or by the application of an external field. Experimentally, this mechanism might be obtained by enclosing the whole chain of colloids into a semiflexible steric casing, with no actual crosslinks between the particles. This model is also the first step from a self-assembled chain to a permanently bound magnetic filament, and it allows us to study separately the contribution of the magnetic dipole-dipole interactions to the collective behaviour of permanently linked particles.

2.3 Chain connectivity Model 2: bond-dipole coupling model

The most common synthesis techniques of magnetic filaments are based on the crosslinking of magnetically assembled colloids by means of polymers. In such approach, the ends of the polymer chains are chemically bonded to the surface of the linked colloids. Therefore, the crosslinking polymers not only constrain the interparticle distance, but also their relative orientations. For the case of ferromagnetic colloids, with the dipole moment fixed within the particle crystallographic axes, the constraints imposed by the crosslinkers are unavoidably extended to the relative orientation of the magnetic dipoles. To date, the knowledge on the effects of the experimental crosslinkers on the internal degrees of freedom of the chains and their overall mechanical properties is still basically qualitative. For instance, it is known that the experimental flexibility of the links depends on the nature of the used polymers, their amount and their lengths,[27] but no accurate description exists to our best knowledge. Therefore, we choose a simple phenomenological approach to define our linking potential. In a previous work, we introduced the following expression for a pair potential that links the surfaces of two ferromagnetic colloids:[36]

$$U_S(\vec{r}_{ij};\hat{\mu}_i,\hat{\mu}_j) = \frac{1}{2}K_S\left(\vec{r}_{ij} - (\hat{\mu}_i + \hat{\mu}_j)\frac{\sigma}{2}\right)^2, \qquad (5)$$

where $\hat{\mu}_i = \vec{\mu}_i / \|\vec{\mu}_i\|$ and $\hat{\mu}_j = \vec{\mu}_j / \left\|\vec{\mu}_j\right\|$ are the unitary vectors parallel to each associated dipole moment. As Figure 1(b) illustrates, this potential represents the constraining effects of the crosslinkers that bond any pair of neighbouring beads as a simple harmonic spring whose ends are attached to the 'surface' of both soft spheres, *i.e.*, to points at a distance $\sigma/2$ from the sphere centres. Assuming that the equilibrium position for the crosslinkers is a perfect head-to-tail alignment of both dipoles at a centre-to-centre separation distance σ, the combination of this bonding potential with the steric repulsions, defined by (2), will penalise the stretching of the links produced either by an increase of the centre-to-centre separation of the beads, or by rotations that lead to a non head-to-tail alignment of the dipoles. It should be noted that the added bond stretching that one may expect for large misalignments of adjacent dipoles, assuming that the springs can not freely penetrate the core of the beads, is not taken into account in this model. However, such large misalignments are expected to be exclusively associated with highly entropic conditions and, therefore, their effects can be disregarded in this study. According to our previous work,[36] the prefactor of the potential is set to $K_s = 30$, a value that again is expected to provide bond lengths close to the reference bead soft core diameter, $\sigma = 1$. In difference with such previous study, devoted to the qualitative determination of the the structural phase diagram of a single magnetic filament under poor solvent conditions, here we assume good solvent conditions and, therefore, we do not introduce any isotropic attractive potential between the colloids.

3 Simulation and Analytical methods

3.1 Computer simulation methods

Extensive computer simulations for both filament models were performed by means of the Langevin dynamics method (LD), which treats implicitly the effects of the thermal fluctuations of the carrier fluid on the dipolar beads.[40] This was combined with the replica exchange molecular dynamics method (REMD), a technique designed to ease the proper equilibration of systems with a complex free energy landscape by preventing the simulation from becoming trapped into local energy minima.[41,42]

In LD simulations each particle i follows the translational and rotational Langevin equations of motion:

$$\begin{aligned} m_i \frac{d\vec{v}_i}{dt} &= \vec{F}_i - \Gamma_T \vec{v}_i + \vec{\xi}_{i,T}, \\ \vec{I}_i \cdot \frac{d\vec{\omega}_i}{dt} &= \vec{\tau}_i - \Gamma_R \vec{\omega}_i + \vec{\xi}_{i,R}, \end{aligned} \tag{6}$$

where $\vec{F}_i$, and $\vec{\tau}_i$ are respectively the total force and torque acting on the particle. m_i is its mass, $\vec{I}_i$ its inertia tensor, and Γ_T and Γ_R the translational and rotational friction constants. Finally, $\vec{\xi}_{i,T}$ and $\vec{\xi}_{i,R}$ are a Gaussian random force and torque, respectively, each of zero mean and satisfying the usual fluctuation-dissipation relations. Since here we are only interested in the equilibrium properties of the system, the values of the dynamical parameters—*i.e.*, the values of the mass, the inertia tensor, and the friction constants—are physically irrelevant. Thus, we have taken $\Gamma_T = 1$ and $\Gamma_R = 3/4$ as values known to produce a conveniently fast relaxation to equilibrium in these types of simulations.[43,44] Finally, in order to ensure isotropic rotations, we take the inertia tensor to be the identity matrix.

The combination of the LD and REMD methods was performed in the following way. First, a set of M reduced temperatures spanning a range of interest, $\{T_M\} = \{T_1 < T_2 < \cdots < T_M\}$, was chosen from some preliminary test runs by imposing a replica exchange acceptance ratio not lower than 30%. For each temperature, an independent canonical LD simulation, or replica, was started by placing a filament, created as a self-avoiding random walk of N beads with squared dipolar moment μ^2, in a simulation box with open boundaries. The initial pre-equilibration run for each replica was then performed, consisting in $5 \cdot 10^5$ integration steps at $T = 2$ and $\mu^2 = 0$, using a timestep of $1 \cdot 10^{-6}$. Then the temperature was set to the value given to the corresponding replica, the timestep was increased to $1 \cdot 10^{-3}$ and the dipole moments set to the desired value. From this point, a number of equilibration-measures cycles of $1 \cdot 10^7$ integration steps each was carried out. Measures of the system parameters were obtained during the second part of every cycle at intervals of $1 \cdot 10^6$ integration steps. After the completion of every cycle, an attempt to exchange the system configurations of different replicas with adjacent temperatures in the set was performed according to the probability $P_{a \leftrightarrow b} = \min(1, \exp[-(1/T_b - 1/T_a)(U_a - U_b)/k])$, where U_i is the total potential energy of the replica with temperature T_i. In general, no less than 1500 cycles were performed for every model and selected values of chain length and dipole moment, and at least the first 300 cycles were discarded for the final calculation of equilibrium averages. All of the simulations were made with the package ESPResSo 3.2.0.[45,46] The measured parameters were the average centre-to-centre distance and dipole-dipole correlation coefficient between first-nearest neighbour particles, and the mean squared net magnetic moment of the chain. The average centre-to-centre distance between first-nearest neighbours, or bond length, is defined as

$$\langle b \rangle = \langle \| \vec{r}_i - \vec{r}_{i+1} \| \rangle , \tag{7}$$

where the average $\langle \cdot \rangle$ was carried out over every pair of neighbouring particles ($i = 1, \ldots, N-1$), and over every measured chain configuration. The same averaging was made for the dipole-dipole correlation coefficient, which is obtained from the scalar product of the unitary dipole moments of every pair of neighbouring dipoles,

$$\langle C_{dd} \rangle = \langle \hat{\mu}_i \cdot \hat{\mu}_{i+1} \rangle . \tag{8}$$

Finally, the average squared net magnetic moment is calculated as the squared vector sum of the dipolar moments along the whole chain, averaged over every measured chain configuration,

$$\langle M^2 \rangle = \left\langle \left(\sum_{i=1}^{N} \vec{\mu}_i \right)^2 \right\rangle . \tag{9}$$

These observables will help to analyse in detail the intrachain correlations.

3.2 Analytical approach

The self-assembly of magneitc dipolar particles has been extensively studied by means of various analytical models.[47–58] Commonly these models are based on the density functional theory. In this approach, the self-assembly of the magnetic colloids into dipolar aggregates is characterised by the minimisation of the free energy of the system, which is defined as a functional of the cluster distribution density. Following Wertheim's theory[59] or the theory of heterophase fluctuations of Frenkel,[60] the free energy density functional is usually split into two terms. The first term represents the entropy of an ideal gas of formed clusters, whereas the second term (and where the main challenge is located) is responsible for the free energy of a single cluster. Ideally, the partition function of a cluster comprises all interparticle inter-

actions between the member particles. When these interactions are patchy-like one can treat them accurately.[61] However, if one of those interactions is the long-range dipole-dipole one, significant simplifications and restrictive assumptions are required to make the problem tractable. Rather significant progress has been achieved in these calculations in recent years, albeit, the restriction to the first nearest neighbours interactions (FNN) within the cluster still remains almost unavoidable. Another simplification frequently used in analytical approaches for magnetic fluids is the consideration of the magnetic colloids as ideal dipolar hard spheres (DHS). Here, we only used the FNN approximation in our calculation of the filament partition function, which is particularly complicated due to the presence of the spring bonding potentials introduced above.

Here, we use the previously developed formalism to estimate the magnetic response of a self-assembled ferroparticle chain.[53,56] We generalise it to calculate the mean squared net magnetic moment of a filament, which is the main contribution to its zero field magnetic susceptibility. Assuming the FNN approximation and zero external field conditions, the following general expression can be obtained for the average squared net magnetic moment of a dipolar chain of N spheric magnetic colloids, measured in units of μ^2:[56]

$$\langle M^2 \rangle = N + \frac{2C_{dd}}{(1-C_{dd})^2}\left[N-1+C_{dd}^N - NC_{dd}\right], \quad (10)$$

where C_{dd} is the correlation coefficient of two neighbouring dipoles in the chain. In order to obtain this coefficient, one needs to calculate the weighted statistical average of the neighbouring dipoles' scalar product taking into account all interparticle interactions.

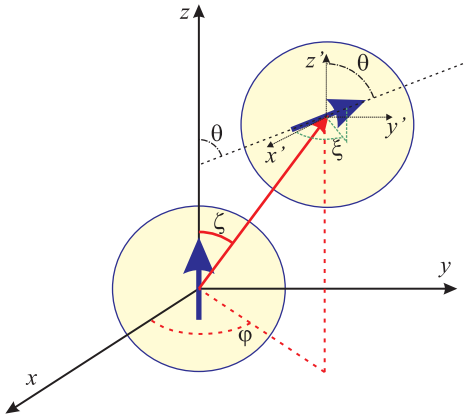

Fig. 2 Coordinate system used in our analytical calculations.

In general terms, the Hamiltonian of the system can be presented as a sum of bonding and dipolar contributions, $U_b + U_{dd}$, where U_b stands for $U_b = U_{\mathrm{WCA}} + U_{\mathrm{FENE}}$ in Model 1 and $U_b = U_{\mathrm{WCA}} + U_S$ in Model 2. In the former model the angular dependence of the Hamiltonian stays only in the dipolar part, whereas in the latter there is also an angular dependence in U_b. Figure 2 shows the coordinate system and the angle definitions used in our calculations. In both models, the dependence of the Hamiltonian on the angles φ, ξ and ζ can be integrated out analytically. As a result, rather compact expressions for the average bond length, dipolar correlation coefficient and mean squared net magnetic moment can be obtained from the partition function of two neighbouring dipoles. The expression for the bond length has the form

$$\left\langle b^{(i)}(T)\right\rangle = \frac{\int_{r_{min}}^{r_{max}} dr \int_0^{\pi} d\theta\; r\, q^{(i)}(r,\theta,T)}{\int_{r_{min}}^{r_{max}} dr \int_0^{\pi} d\theta\; q^{(i)}(r,\theta,T)}, \quad (11)$$

where index $i \in \{1,2\}$ denotes the number of the model, r_{min} and r_{max} are the boundaries of the interval of bond lengths allowed by the respective bonding potential well, and the expression in the denominator is the aforementioned partition function of two neighbouring dipoles, with $q^{(i)}$ being the integrand obtained after integrating out ϕ-, ξ- and ζ-dependence. Analogously, the general expression for the correlation coefficient has the form

$$\left\langle C_{dd}^{(i)}(T)\right\rangle = \frac{\int_{r_{min}}^{r_{max}} dr \int_0^{\pi} d\theta\; p^{(i)}(r,\theta,T)}{\int_{r_{min}}^{r_{max}} dr \int_0^{\pi} d\theta\; q^{(i)}(r,\theta,T)}. \quad (12)$$

For Model 1, $q^{(1)}$ is defined as

$$q^{(1)} = r^2 \exp\left(-\frac{U_{\mathrm{WCA}}(r)+U_{\mathrm{FENE}}(r)}{T}\right)\sin\theta \times \\ \times \frac{\sinh x(\theta)}{x(\theta)}, \quad x(\theta) = \frac{\lambda}{r^3}\sqrt{3\cos^2\theta+1}, \quad (13)$$

where $\lambda \equiv \mu^2/T\sigma^3$ is the usual dipolar coupling parameter for spherical colloids. For the same model, $p^{(1)}$ is defined as

$$p^{(1)} = r^2 \exp\left(-\frac{U_{\mathrm{WCA}}(r)+U_{\mathrm{FENE}}(r)}{T}\right)\sin\theta \times \\ \times \frac{\lambda}{r^3 x(\theta)^3}\left(3\cos^2\theta-1\right) \times \\ \times \left[x(\theta)\cosh x(\theta) - \sinh x(\theta)\right]. \quad (14)$$

According to our choices for Equations (2) and (4), the integration limits are in this case $r_{min} \lesssim r_{cut} = 2^{1/6}$ and $r_{max} = r_f = 1.5$.

One can write analogous expressions for Model 2,

$$q^{(2)}(r,\theta,T) = r^2 \exp\left(-\frac{U_{\mathrm{WCA}}(r)}{T}\right)\frac{\sinh A}{A}\times \\ \times \exp\left(-\frac{K}{2T}\left[r^2+\frac{1}{2}-r\cos\theta\right]\right), \\ A = A(r,\theta,T) = \left[\frac{1}{4}\frac{K_S^2}{T^2}\left(r^2+\frac{1}{4}-r\cos\theta\right)+ \right. \\ \left. +x(\theta)^2+\frac{K_S\lambda}{Tr^2}\left(2\cos\theta-\frac{3\cos^2\theta-1}{2r}\right)\right]^{1/2}, \quad (15)$$

and

$$p^{(2)}(r,\theta,T) = r^2 \exp\left(-\frac{U_{\mathrm{WCA}}(r)}{T}\right)\frac{B}{A^3}\times \\ \times \exp\left(-\frac{K}{2T}\left[r^2+\frac{1}{2}-r\cos\theta\right]\right)\left[A\cosh A-\sinh A\right], \\ B = B(r,\theta,T) = \frac{K_S}{2T}\left(r\cos\theta-\frac{1}{2}\right)+ \\ +\frac{\lambda}{r^3}\left(3\cos^2\theta-1\right). \quad (16)$$

Finally, for this model the integration limits are $r_{min} \lesssim r_{cut} = 2^{1/6}$ and $r_{max} = \infty$.

We should keep in mind the limitations inherent to this approach. In particular, the FNN approximation will make the theory more inaccurate as the value of the squared modulus of the dipole moment of the colloids, μ^2, grows in relation to their centre-to-centre separation distance and the thermal fluctuations, which grow with the reduced temperature, T. In terms of the dipolar coupling parameter, we expect our analytical theory to be accurate only for low and intermediate values of λ, since the effects of the second and further nearest neighbours on the orientational correlations of the dipoles will grow with such a parameter. In addition, we expect that filaments will form closed rings at high values of λ,[36,39] analogously to the behaviour observed for self-assembled dipolar chains,[7,62–71] completely invalidating expression (10). On the other hand, at very high temperatures any correlation between the dipoles in both models will tend to fade out, making the behaviour of the net magnetic moment of the chains trivial. For Model 1, where there is no mechanism to drive orientational correlations other than the dipolar interaction, both high temperatures and/or low dipolar moments may hinder such correlations. Therefore, we restricted ourselves to the range $\lambda \in [0.4, 2.0]$ approximately, by sampling reduced temperatures with values up to $T \leq 2.5$, whilst keeping $\mu^2 = 1.0$ for simplicity. The explored chain lengths have been also limited to the range $N \in [2, 50]$.

4 Results and discussion

4.1 Model 1

The result of the numerical integration of Equations (11) and (14), together with some selected simulation results for this model, is shown in the main plot of Figure 3. For a chain of just two particles, the agreement between the analytical results and the simulation data is excellent for the whole range of sampled temperatures. For longer chains, however, there are slight but systematic deviations that point to the existence of two different regimes. At low temperatures, $T < 0.65$, the average bond length tends to slightly decrease with the chain length. This may be explained by the additional attractive dipolar force coming from second and further nearest neighbours in the chain at low temperatures, which is not taken into account by the analytical model. As T decreases, the dipoles tend to be more well aligned with the chain backbone, adopting locally straight head-to-tail arrangements, whereas at high temperatures the orientations of the dipoles tend to be disordered.[39] This explanation is supported by the inset plot of Figure 3 that shows the dipole-dipole correlation function, defined as $g_{dd}(k) = \langle \vec{\mu}_i \cdot \vec{\mu}_{i+k} \rangle_{i=1,\ldots,N;\,\mathrm{run}}$, for $N = 50$ and some selected temperatures. It can be observed that at $T = 0.4$ the correlation between the dipoles is still significant for the second, third and even fourth nearest neighbours. Remarkably, $T \sim 0.65$ corresponds approximately to the temperature at which correlations for positions beyond first nearest neighbours become insignificant. Therefore, as a rough criterium, we consider $T < 0.65$ (or, more generally, $\lambda > 1.5$) the region where the FNN approximation becomes inaccurate for this model. This value is much lower than that for self-assembling magnetic particles.[44] Finally, at $T > 0.65$ the deviations between the analytical model and the simulation results for the average bond length are reversed: here this parameter grows slightly more with the chain length. In this case, the weak direct dependence of $\langle b \rangle$ on N cannot be related to the dipolar interactions, since at high temperatures they become basically irrelevant. Instead, this effect should be attributed to the chain entropy, which is not taken into account in the theoretical approach.

Figure 4 shows the result of the integration of Equations (11), (15) and (16), and how it compares to the simulations performed for the same chain lengths selected above. The plot also includes the correlation coefficient of self-assembled dipolar chains in the DHS approximation. This parameter is calculated from the closed expression obtained in the limit of strong dipolar coupling regimes,[56]

$$C_{dd}^{(\mathrm{DHS})} = \coth\left(\frac{\mu^2}{2T\langle b\rangle^3}\right) - \frac{2T\langle b\rangle^3}{\mu^2}, \quad (17)$$

where $\mu^2/T\langle b\rangle^3 \gg 1$ and $\langle b \rangle$ takes the values of average bond

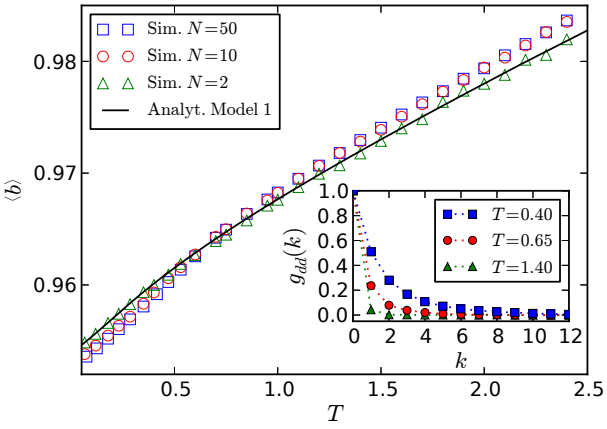

Fig. 3 Main figure: average bond length, $\langle b \rangle$, as a function of the reduced temperature obtained for Model 1 and $\mu^2 = 1.0$. Solid line corresponds to analytical calculations and symbols to simulation data for three different chain lengths: N=2, 10, 50. Error bars for simulation data are of the order of symbol size. Inset figure: dipole orientation pair correlation function obtained from simulation data for $\mu^2 = 1.0$, $N = 50$ and three selected reduced temperatures.

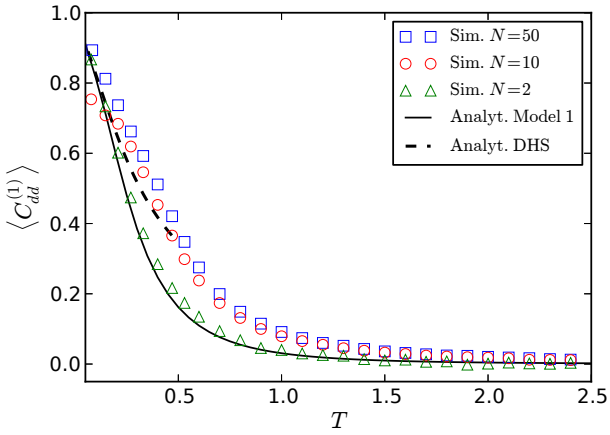

Fig. 4 First-nearest neighbours average correlation coefficient for the orientation of the dipoles as a function of the reduced temperature obtained for $\mu^2 = 1.0$. Solid line corresponds to the analytical theory for Model 1, and dashed line to dipolar chains in the DHS approximation. Symbols represent simulation data for Model 1 and different chain lengths. Error bars are of the order of symbol size.

length given by Equations (11) and (14). The agreement between our analytical theory and the simulation results for the two particles chain is also excellent in this case. In the limit of low temperatures, *i.e.*, the region where C_{dd} is close to its saturation value, our analytical and simulation results for very short and long chains tend to converge to that of the DHS. For intermediate chain lengths, as in the case of $N = 10$, we can see a kink corresponding to the increased dipole misalignments introduced by the formation of closed rings. For $N > 2$ and intermediate temperatures, a difference between the analytical theory and the simulations can also be observed. This difference underlines the importance of long-range interactions for the correlation in this region. In other words, for this model the magnetic dipole-dipole interaction plays a decisive part in the macroscopic response of the filament. Finally, at high temperatures the dipole correlations tend to vanish and the correlation coefficient for any chain length can be well described by the theory, assuming the FNN approximation.

The squared net magnetic moment per particle for Model 1 filaments, obtained from the analytical theories and simulations, is shown in Figure 5. The results for the DHS model were obtained by inserting Equation (17) into Equation (10). The same analytical procedure is applied to Equations (12) and (10) in order to obtain the results for our analytical model. The simulation data shows that the magnetic moment of the chains has a clear maximum at around $T \sim 0.25$ (corresponding to $\lambda \sim 4$). At lower temperatures the chains undergo the closure structural transition associated with the formation of rings, which drastically reduce the net dipole moment and make it tend to zero as the temperature decreases.[35,39] At higher temperatures, the zero field magnetic susceptibility strongly depends on the chain length and the long-range dipolar interactions. This can be seen from growing deviations between the analytical model and simulation data. Finally, for the high temperature regime, where the dipole-dipole interaction becomes irrelevant, the squared magnetic moment per particle tends asymptotically to the value corresponding to a completely random distribution of dipole orientations, $\langle M^2 \rangle / N \to 1$. Concluding this Section, we want to underline that the decorrelation of the dipoles in the filament with growing temperature, despite being much weaker than that in a self-assembled chain, is the consequence of the absence of constraints on particle rotations rather than those imposed by magnetic dipole-dipole interactions. This will change drastically in Model 2.

4.2 Model 2

Figure 6 compares the results of the integration of Equations (11), (15) and (16) with the corresponding simulation data obtained for several chain lengths. The agreement between the analytical results and the simulation data for N=2 is once more excellent. For longer chains a slight difference can also be spotted, in this case as a consequence of the long-range nature of the dipole-dipole interaction. However, in contrast to Model 1, the dependence of the bond length on the number of particles just tends to vanish as the temperature increases and no reversion of such dependence can be observed within the

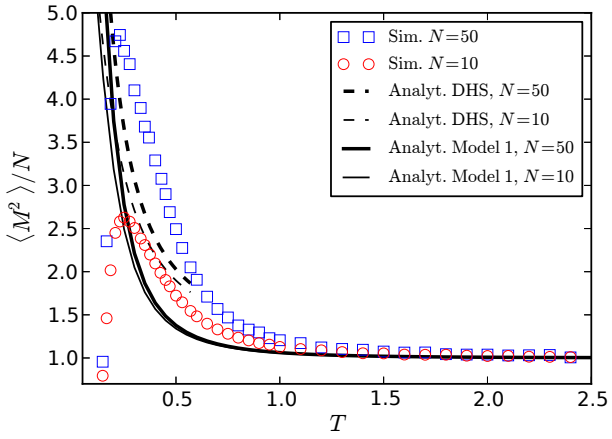

Fig. 5 Average squared net magnetic moment per particle of chains with lengths N=10, 50, and $\mu^2 = 1.0$, plotted as a function of the reduced temperature. Solid lines correspond to our Model 1 analytical theory, dashed lines to the DHS theory, and symbols to Model 1 simulation data. Error bars are of the same order of symbol size.

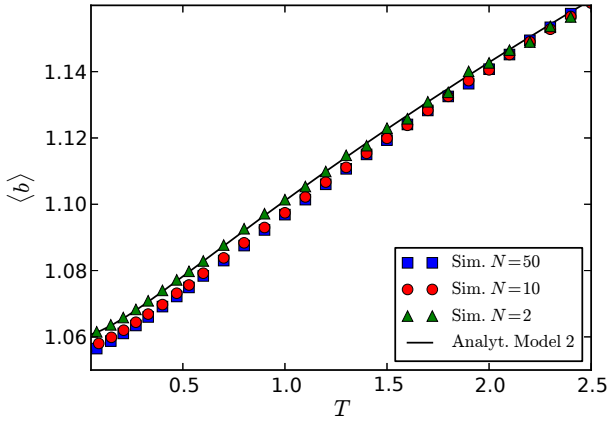

Fig. 6 Average bond length for Model 2 as a function of the reduced temperature, for $\mu^2 = 1.0$. Solid line corresponds to the Model 2 analytical theory and symbols to the simulation data obtained for three different chain lengths. Error bars are of the same order of symbol size.

sampled interval. This is the result of the increased rigidity of Model 2 chains led by the angular bonding potential, which drives to a reduction of the chain bending entropy.

Figure 7 shows the correlation coefficients calculated from Equations (12), (15) and (16) together with the simulation data obtained for different chain lengths according to (8). In order to show how much the elastic bonding potential that links the particles in this model increases their orientational correlations independently from the strength of the dipolar interactions, we also plot the results for $\mu^2 = 0$. This corresponds to the absence of interparticle dipole-dipole interactions and is of particular interest in the case of magnetisable particles. As expected, the analytical results agree very well with the simulation data for the two particles chain and for both $\mu^2 = 0$ and $\mu^2 = 1$. For longer chains, a slight underestimation of the correlation can be observed. However, in contrast to the results of Model 1, here the assumption of FNN is shown to work much better. The reason for this satisfactory result is that here the dipolar correlations, in larger part, are stimulated by the orientational bonding. This bonding in its turn is a local property of each neighbours pair and has no explicit long-range character. Thus, the theoretical formalism presented in this work can be safely used to predict the zero field magnetic susceptibility of Model 2 filaments. Figure 8 confirms this point. In this Figure, one can see that the local rigidity of chains inhibits the closure structural transition, so that the drop of the net squared magnetic moment is observed at much lower temperatures, especially for short chains. The difference in magnetic response between theory and simulations is rather small, and can be still attributed to the increase of the chain degrees of freedom with growing N. Another important conclusion to be drawn from this plot is how the DHS approximation provides not only a quantitatively, but also a qualitatively inaccurate picture of the magnetic response in this case.

5 Concluding remarks

In this work we presented the study of the zero field correlations of colloids within differently linked supramolecular magnetic filaments. We employed Langevin dynamics simulations and analytical theories to characterise the initial susceptibility in the framework of two distinct models. In the first model, magnetic beads were connected by a FENE potential constraining the interparticle separation but not the particle rotations. It turns out that for such filaments the interparticle correlations are highly sensitive to the long-range character of the magnetic dipole-dipole interaction. This dependence manifests itself more strongly than in self-assembled dipolar chains. This conclusion follows from the fact that the analytical approach, which for self-assembled particles demonstrates a very good agreement with the simulation data for the initial susceptibility, in this case fails for any filament longer than two particles. In the second model, the bonding potential not only constrains the interparticle separation, but also penalises the rotation of the dipoles out of a locally straight head-to-tail orientation. In this case, the behaviour of the filaments is mainly determined by the orientational bonds. Being short ranged, these bonding interactions act locally, which results in two characteristic properties of Model 2 filaments. Firstly, the interparticle correlations are barely dependent on the chain length, which makes the theoretical approach fully applicable.

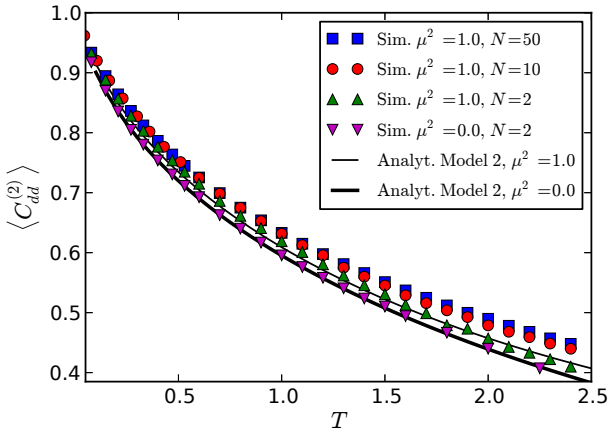

Fig. 7 First-nearest neighbours average correlation coefficient for the orientations of the dipoles in Model 2 chains as a function of the reduced temperature. Solid lines correspond to the analytical Model 2 theory for two values of the dipolar moment. Symbols represent the simulation results for three different chain lengths. Error bars are of the order of symbol size.

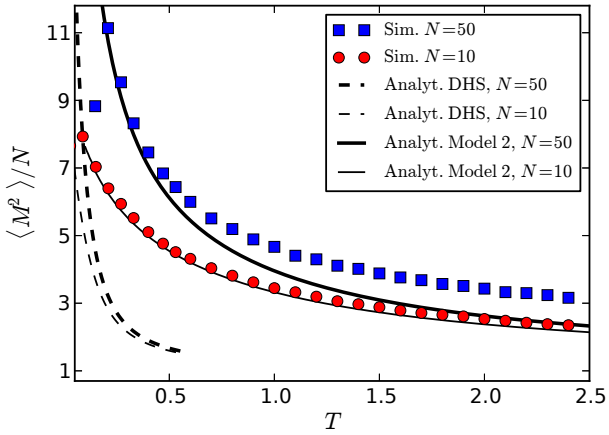

Fig. 8 Average squared net magnetic moment per particle of Model 2 chains for $\mu^2 = 1$ as a function of the reduced temperature. Simbols correspond to simulation data, solid lines to the analitycal Model 2 theory, and dashed lines to the DHS theory. Error bars are of the same order of symbol size.

Secondly, the high temperature interparticle dipolar correlations are still pronounced, leading to a much higher zero field magnetic susceptibility. In this way, the linking mechanism of the particles in chains can be used as a control parameter to tune the magnetic response of the supramolecular magnetic filaments.

It is worth noting here that Model 2 is phenomenologically closer to the most common available experimental techniques for the synthesis of magnetic filaments. This suggests that the simple theoretical model developed here could be fitted to describe the thermodynamic properties of a system of magnetic filaments. As for the analytical description in Model 1, further improvement can be done either by introducing the contribution of the next nearest neighbours interactions, or alternatively by using the mean field approach. Both of these extensions deserve a separate study. Another possible extension of this work is to scrutinise the influence of the elastic constants in Model 2, which is the subject of a work in progress. Finally, a detailed study on the structural closure of magnetic filaments and its analysis on the basis of the theory developed for the self-assembled rings found in dispersions of free magnetic colloids [7] will be completed soon.

Acknowledgements

PS and SK acknowledge financial support from the START Project Y 627-N27 of the Austrian Science Fund (FWF). TS and JC acknowledge project FIS2012-30634 (funded by the Spanish Mineco). This research was also supported by the Ural Federal University stimulating programme and by the Ministry of Education and Science of the Russian Federation (Contract 02.A03.21.000, Project 3.12.2014/K). Computer simulations were performed at the Vienna Scientific Cluster (Austrian universities consortium for High Performance Computing) and the Nuredduna high-throughput computing cluster (IFISC, UIB-CSIC).

References

1 C. Holm and J.-J. Weis, *Curr Opin Colloid Interface Sci*, 2005, **10**, 133–140.
2 *Colloidal Magnetic Fluids*, ed. S. Odenbach, Springer-Verlag, Berlin Heidelberg, 2009, vol. 763.
3 J. de Vicente, D. J. Klingenberg and R. Hidalgo-Alvarez, *Soft Matter*, 2011, **7**, 3701–3710.
4 M. Klokkenburg, C. Vonk, E. M. Claesson, J. D. Meeldijk, B. H. Erné and A. P. Philipse, *J Am Chem Soc*, 2004, **126**, 16706–16707.
5 M. Klokkenburg, R. P. A. Dullens, W. K. Kegel, B. H. Erné and A. P. Philipse, *Phys. Rev. Lett.*, 2006, **96**, 037203.
6 L. Rovigatti, S. Kantorovich, A. O. Ivanov, J. M. Tavares and F. Sciortino, *The Journal of Chemical Physics*, 2013, **139**, 134901.
7 S. Kantorovich, A. O. Ivanov, L. Rovigatti, J. M. Tavares and F. Sciortino, *Phys. Rev. Lett.*, 2013, **110**, 148306.
8 E. Bianchi, G. Kahl and C. N. Likos, *Soft Matter*, 2011, **7**, 8313–8323.
9 Z. Preisler, T. Vissers, G. Munao, F. Smallenburg and F. Sciortino, *Soft Matter*, 2014, **10**, 5121–5128.
10 F. Smallenburg, L. Filion and F. Sciortino, *Nat. Phys.*, 2014, **10**, 653–657.
11 M. Nakata, G. Zanchetta, B. D. Chapman, C. D. Jones, J. O. Cross, R. Pindak, T. Bellini and N. A. Clark, *Science*, 2007, **318**, 1276–1279.
12 G. Zanchetta, F. Giavazzi, M. Nakata, M. Buscaglia, R. Cerbino, N. A. Clark and T. Bellini, *Proceedings of the National Academy of Sciences*, 2010, **107**, 17497–17502.
13 S. Kantorovich, E. Pyanzina, C. De Michele and F. Sciortino, *Soft Matter*, 2013, **9**, 4412–4427.

14 L. Rovigatti, F. Smallenburg, F. Romano and F. Sciortino, *ACS Nano*, 2014, **8**, 3567–3574.

15 Z. Shulman, V. Kordonsky, E. Zaltsgendler, I. Prokhorov, B. Khusid and S. Demchuk, *International Journal of Multiphase Flow*, 1986, **12**, 935–955.

16 B. J. Park, F. F. Fang and H. J. Choi, *Soft Matter*, 2010, **6**, 5246–5253.

17 S. Frank and P. C. Lauterbur, *Nature*, 1993, **363**, 334–336.

18 M. Zriñyi, D. Szabó and H.-G. Kilian, *Polymer Gels and Networks*, 1998, **6**, 441–454.

19 R. Weeber, S. Kantorovich and C. Holm, *Soft Matter*, 2012, **8**, 9923–9932.

20 P. W. K. Rothemund, *Nature*, 2006, **440**, 297–302.

21 S. Pal, Z. Deng, B. Ding, H. Yan and Y. Liu, *Angewandte Chemie*, 2010, **122**, 2760–2764.

22 R. M. Zadegan and M. L. Norton, *International Journal of Molecular Sciences*, 2012, **13**, 7149–7162.

23 R. Dreyfus, J. Baudry, M. L. Roper, M. Fermigier, H. A. Stone and J. Bibette, *Nature*, 2005, **437**, 862–865.

24 J. J. Benkoski, S. E. Bowles, R. L. Jones, J. F. Douglas, J. Pyun and A. Karim, *J Polym Sci, Part B: Polym Phy*, 2008, **46**, 2267–2277.

25 K. Ērglis, D. Zhulenkovs, A. Sharipo and A. Cēbers, *J Phys-Condens Mat*, 2008, **20**, 204107.

26 Z. Zhou, G. Liu and D. Han, *ACS Nano*, 2009, **3**, 165–172.

27 J. Byrom, P. Han, M. Savory and S. L. Biswal, *Langmuir*, 2014, **30**, 9045–9052.

28 D. Sarkar and M. Mandal, *The Journal of Physical Chemistry C*, 2012, **116**, 3227–3234.

29 A. Cēbers, *Curr Opin Colloid Interface Sci*, 2005, **10**, 167–175.

30 M. Belovs and A. Cēbers, *Phys Rev E*, 2009, **79**, 051503.

31 F. Fahrni, M. W. J. Prins and L. J. van IJzendoorn, *Lab Chip*, 2009, **9**, 3413–3421.

32 A. Babataheri, M. Roper, M. Fermigier and O. D. Roure, *Journal of Fluid Mechanics*, 2011, **678**, 5–13.

33 I. Javaitis and V. Zilgalve, *Adv Mat Res*, 2011, **222**, 221–224.

34 H. Wang, Y. Yu, Y. Sun and Q. Chen, *Nano*, 2011, **06**, 1–17.

35 P. A. Sánchez, J. J. Cerdà, V. Ballenegger, T. Sintes, O. Piro and C. Holm, *Soft Matter*, 2011, **7**, 1809–1818.

36 J. J. Cerdà, P. A. Sánchez, T. Sintes and C. Holm, *Soft Matter*, 2013, **9**, 7185–7195.

37 J. D. Weeks, D. Chandler and H. C. Andersen, *J Chem Phys*, 1971, **54**, 5237–5247.

38 L. J. Hill and J. Pyun, *ACS Appl. Mater. Interfaces*, 2014, **6**, 6022–6032.

39 P. A. Sánchez, J. J. Cerdà, T. Sintes and C. Holm, *J. Chem. Phys.*, 2013, **139**, 044904.

40 M. P. Allen and D. J. Tildesley, *Computer Simulation of Liquids*, Clarendon Press, Oxford, 1st edn, 1987.

41 Y. Sugita and Y. Okamoto, *Chem. Phys. Lett.*, 1999, **314**, 141–151.

42 A. Mitsutake, Y. Sugita and Y. Okamoto, *Peptide Science*, 2001, **60**, 96–123.

43 J. J. Cerdà, S. Kantorovich and C. Holm, *J Phys-Condens Mat*, 2008, **20**, 204125.

44 S. Kantorovich, J. J. Cerdà and C. Holm, *Phys Chem Chem Phys*, 2008, **10**, 1883–1895.

45 H. J. Limbach, A. Arnold, B. A. Mann and C. Holm, *Comput Phys Commun*, 2006, **174**, 704–727.

46 A. Arnold, O. Lenz, S. Kesselheim, R. Weeber, F. Fahrenberger, D. Roehm, P. Košovan and C. Holm, *Meshfree Methods for Partial Differential Equations VI*, Springer Berlin Heidelberg, 2013, vol. 89, pp. 1–23.

47 A. Y. Zubarev and L. Y. Iskakova, *J. Exp. Theor. Phys.*, 1995, **80**, 857–866.

48 R. P. Sear, *Phys. Rev. Lett.*, 1996, **76**, 2310–2313.

49 M. A. Osipov, P. I. C. Teixeira and M. M. Telo da Gama, *Phys Rev E*, 1996, **54**, 2597–2609.

50 J. M. Tavares, J. J. Weis and M. M. Telo da Gama, *Phys. Rev. E*, 1999, **59**, 4388–4395.

51 J. M. Tavares, J. J. Weis and M. M. Telo da Gama, *Phys Rev E*, 2002, **65**, 061201.

52 A. Zubarev, *Ferrofluids*, Springer Berlin Heidelberg, 2002, vol. 594, pp. 143–161.

53 K. Morozov and M. Shliomis, *Ferrofluids*, Springer Berlin Heidelberg, 2002, vol. 594, pp. 162–184.

54 K. I. Morozov and M. I. Shliomis, *J Phys-Condens Mat*, 2004, **16**, 3807.

55 A. O. Ivanov, Z. Wang and C. Holm, *Phys Rev E*, 2004, **69**, 031206.

56 V. S. Mendelev and A. O. Ivanov, *Phys. Rev. E*, 2004, **70**, 051502.

57 I. Szalai and S. Dietrich, *The European Physical Journal E*, 2009, **28**, 347–359.

58 H. Schmidle, C. K. Hall, O. D. Velev and S. H. L. Klapp, *Soft Matter*, 2012, **8**, 1521–1531.

59 M. S. Wertheim, *The Journal of Chemical Physics*, 1987, **87**, 7323–7331.

60 J. Frenkel, *The Journal of Chemical Physics*, 1939, **7**, 538–547.

61 L. Rovigatti, J. M. Tavares and F. Sciortino, *Phys. Rev. Lett.*, 2013, **111**, 168302.

62 P. de Gennes and P. Pincus, *Zeitschrift für Physik B Condensed Matter*, 1970, **11**, 189–198.

63 A. Ghazali and J.-C. Lévy, *Phys Rev B*, 2003, **67**, 064409.

64 S. L. Tripp, R. E. Dunin-Borkowski and A. Wei, *Angew Chem Int Edit*, 2003, **42**, 5591–5593.

65 A. Hucht, S. Buschmann and P. Entel, *Europhys Lett*, 2007, **77**, 57003.

66 H. Wang, Q.-W. Chen, Y.-B. Sun, M.-S. Wang, L.-X. Sun and W.-S. Yan, *Langmuir*, 2010, **26**, 5957–5962.

67 M. Yoon and D. Tománek, *J Phys-Condens Mat*, 2010, **22**, 455105.

68 A. Wei, T. Kasama and R. E. Dunin-Borkowski, *J Mater Chem*, 2011, **21**, 16686–16693.

69 T. Prokopieva, V. Danilov and S. Kantorovich, *J Exp Theor Phys*, 2011, **113**, 435–449.

70 L. Rovigatti, J. Russo and F. Sciortino, *Soft Matter*, 2012, **8**, 6310–6319.

71 W.-F. Ding, Z. Li, H. Zhou, B. Zhao, J.-g. Wan, F. Song and G.-H. Wang, *J Phys Chem C*, 2012, **116**, 10805–10813.

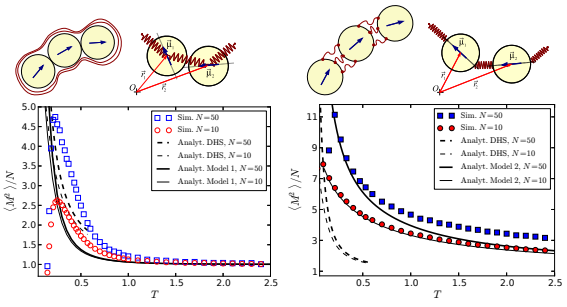

We show theoretically how the crosslinking mechanism of the colloids can drastically change the magnetic response of supramolecular magnetic filaments.